

Metallo- β -lactamases challenge low Zn^{II} conditions by tuning metal-ligand interactions

Javier M. González*^{1,2}, María-Rocío Meini*¹, Pablo E. Tomatis,¹ Francisco J. Medrano
Martín^{3,4}, Julia A. Cricco¹, & Alejandro J. Vila¹

¹ Instituto de Biología Molecular y Celular de Rosario (IBR), Consejo Nacional de Investigaciones Científicas y Técnicas (CONICET), Facultad de Ciencias Bioquímicas y Farmacéuticas, Universidad Nacional de Rosario (UNR), Suipacha 531, S2002LRK Rosario, Argentina. ² Present address: Department of Pharmaceutical Sciences and UMXSS Crystallography Service, University of Maryland at Baltimore, Baltimore, MD 21201, USA. ³ Laboratório Nacional de Luz Síncrotron, Rua Giuseppe Máximo Scolfaro 10000, Campinas, Sao Paulo, CEP 13083-100, Brazil. ⁴ Present address: Centro de Investigaciones Biológicas (CSIC), Ramiro de Maeztu 9, E-28040 Madrid, Spain.

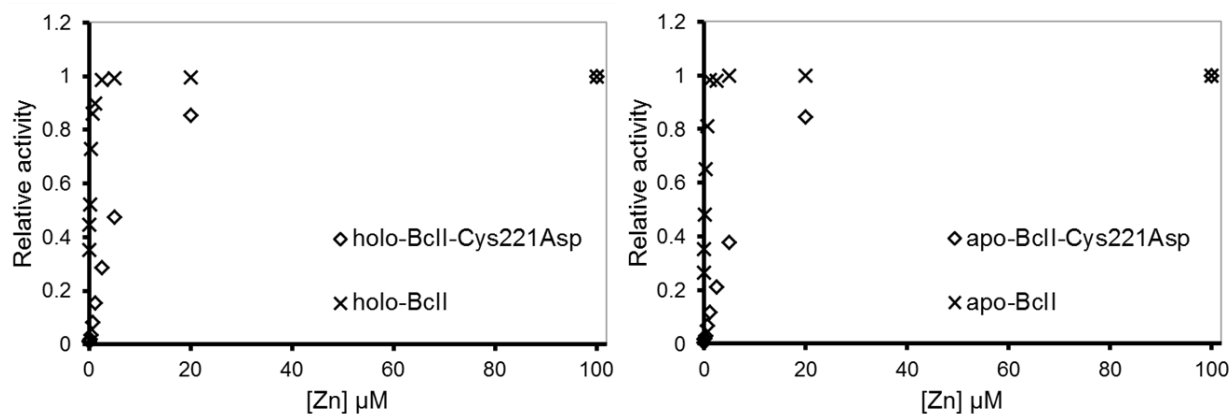
Correspondence should be addressed to JAC (cricco@ibr.gov.ar) and AJV (vila@ibr.gov.ar)

* These authors contributed equally to this paper.

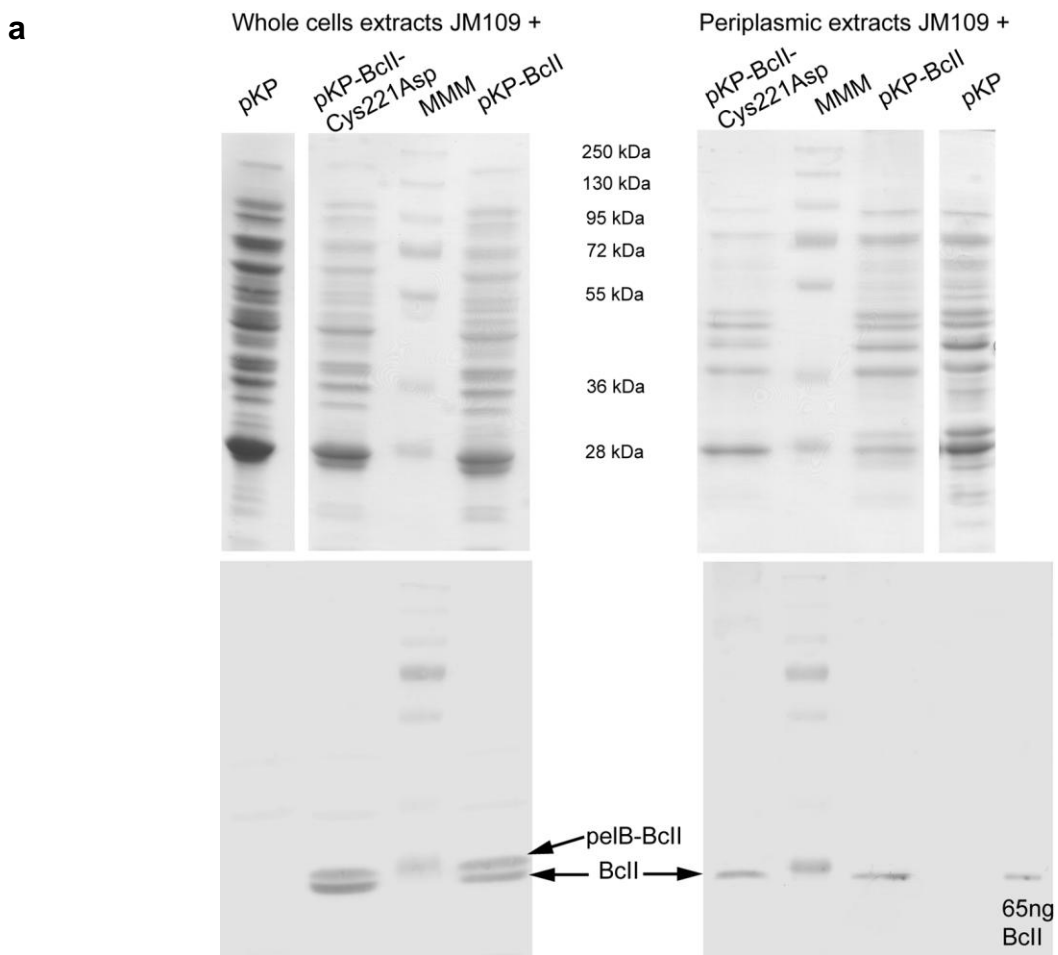
SUPPLEMENTARY INFORMATION

Supplementary Results

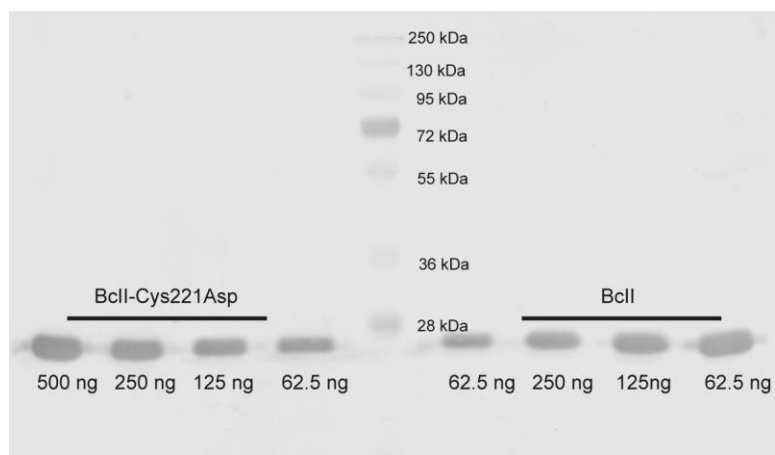
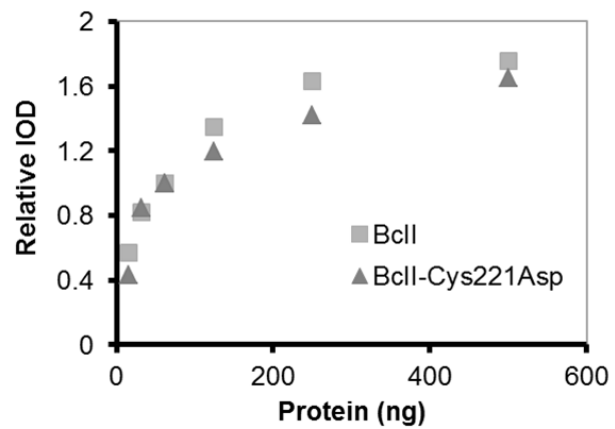
Supplementary Figure 1. Catalytic activity of BcII and BcII-Cys221Asp at increasing Zn^{II} concentrations. Hydrolytic rates under steady state conditions were measured upon dilution of the holo (left panel) and the apo forms (right panel) and further addition of the indicated Zn^{II} concentrations. Reaction rates are reported relative to the value measured at 100 μ M added Zn^{II}. Cefotaxime was used as substrate at a saturating concentration (200 μ M) and final enzyme concentration was 2 nM. Reaction medium: HEPES 15 mM pH 7.5, NaCl 200 mM, at 30°C, previously stirred with Chelex 100. Each point represents the average of three replicates, s.d. were below 5%.



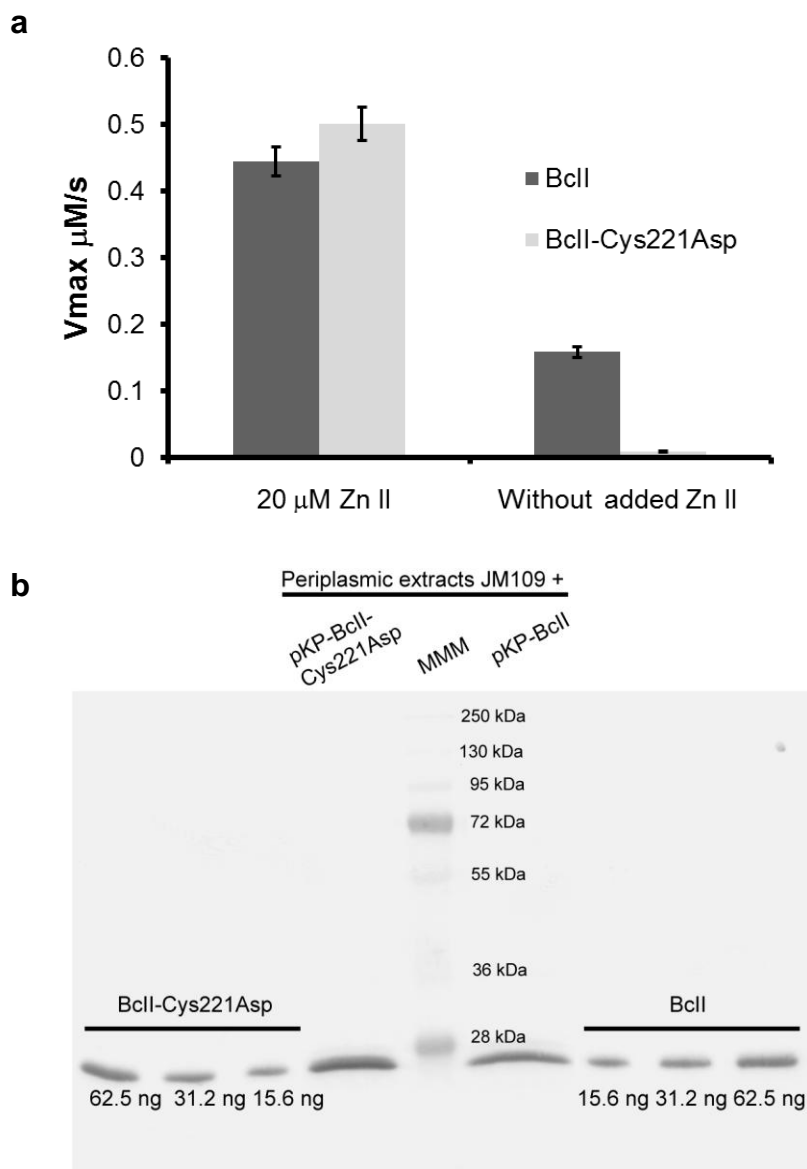
Supplementary Figure 2. Evaluation of expression levels of BcII and BcII-Cys221Asp mutant in *E. coli* cells. (a) SDS-PAGE and Western Blot analysis of whole cell and periplasmic extracts. *E. coli* JM109 cells transformed with pKP, pKP-BcII-Cys221Asp or pKP-BcII were grown and induced with IPTG 0.5 mM. Whole cells extracts and periplasmic extracts were prepared as described previously⁶ and subjected to SDS-PAGE 12 % (upper panel) and Western-blot (lower panel). Western-blot were revealed with rabbit polyclonal antibodies against BcII and alkaline phosphatase-conjugated goat anti-rabbit antibodies (Bio-Rad). Molecular mass markers (MMM, PageRuler™ Plus Prestained Protein Ladder from Fermentas) are indicated. In whole cell extracts the pelB-BcII form (leader peptide plus protein, 27 kDa) and the mature form (25 kDa) are detected, while only the mature form is detected in periplasmic fraction. (b) Calibration of Western blot assays. The reactivity of the anti-BcII polyclonal antibodies was tested for both proteins by using different amounts of purified protein and measuring the intensity of each band by densitometry. The Integrated Optical Density (IOD) of each band was normalized to the band with 62.5 ng in the same assay. See also Supplementary Figure 3.



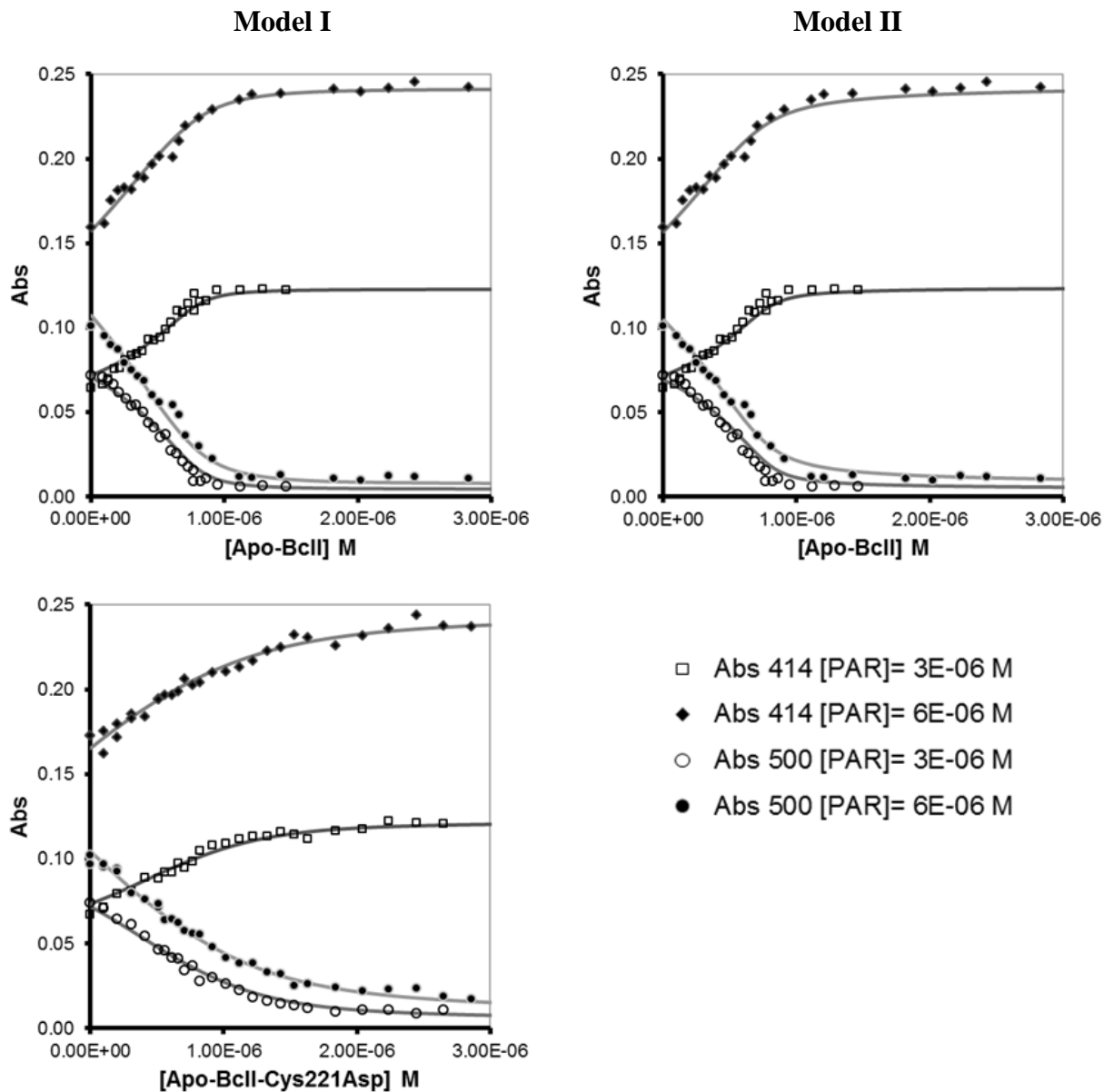
b



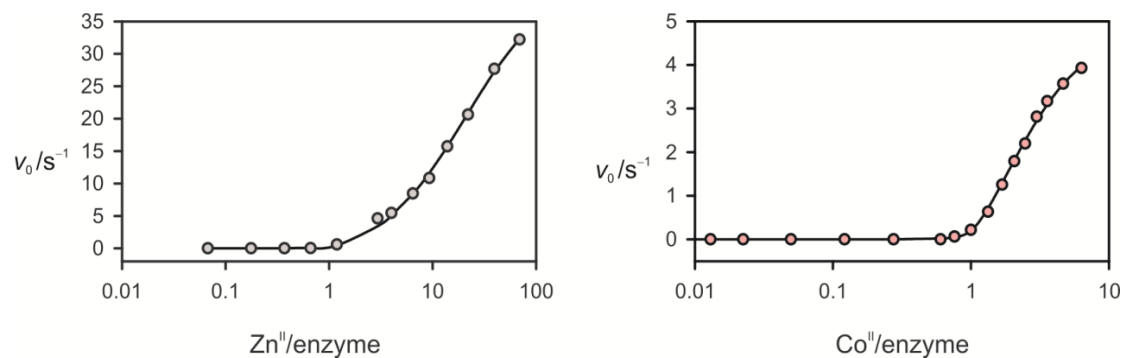
Supplementary Figure 3. Activity measurements with periplasmic extracts. (a) Periplasmic extracts were obtained by osmotic shock as previously described²¹ from *E. coli* JM109 cells expressing either BcII or BcII-Cys221Asp and initial velocities of cefotaxime hydrolysis at saturating substrate concentration were measured. Reaction mediums were: Hepes 15 mM pH 7.5, NaCl 200 mM, at 30°C, previously stirred with Chelex 100, and the same supplemented with 20 μM ZnCl₂. This was repeated with three different periplasmic preparations, error bars represent mean values ± s.d. (b) Quantification of enzyme levels on the periplasmic extracts. Periplasmic extracts and known quantities of purified proteins were loaded on 12 % SDS-PAGE gels and Western blot assays were performed. Measuring the IOD of each band allowed to estimate a concentration of approximately 2 nM for the activity measurements.



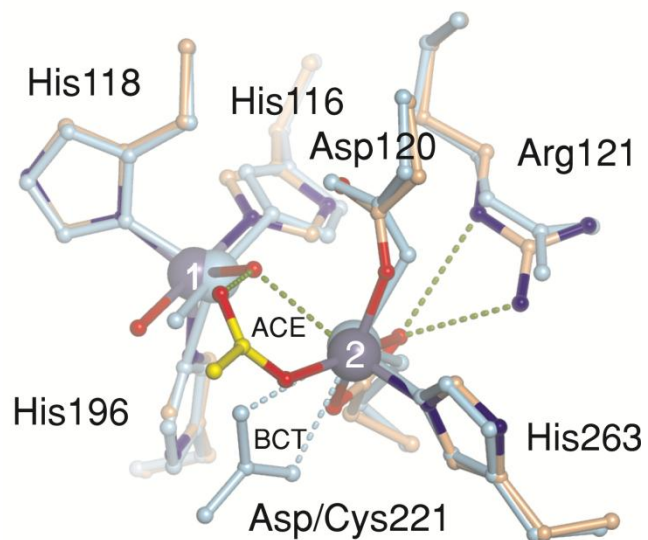
Supplementary Figure 4. Zn^{II} binding affinities for apo-BcII and apo-BcII-Cys221Asp determined by competition assays with PAR (4-(2-pyridylazo)-resorcinol). Increasing concentrations of apo-protein were added to solutions of [Zn]= 1.5 μM and [PAR]= 12 μM or [PAR]= 6 μM. The increase of absorbance at 414 nm reflects the release of free PAR and the decrease of absorbance at 500 nm reflects the disappearance of the (PAR)₂Zn complex. Measurements were performed in Buffer MOPS 40 mM, NaCl 100mM, pH 7.3, previously stirred with CHELEX 100, at 25 °C. Each point represents the average of three replicates, s.d. were below 5%. Data of wild type BcII were fit to Models I and II (see below), while data of Cys221Asp were fit to Model I. Results are summarized in Supplementary Table 2.



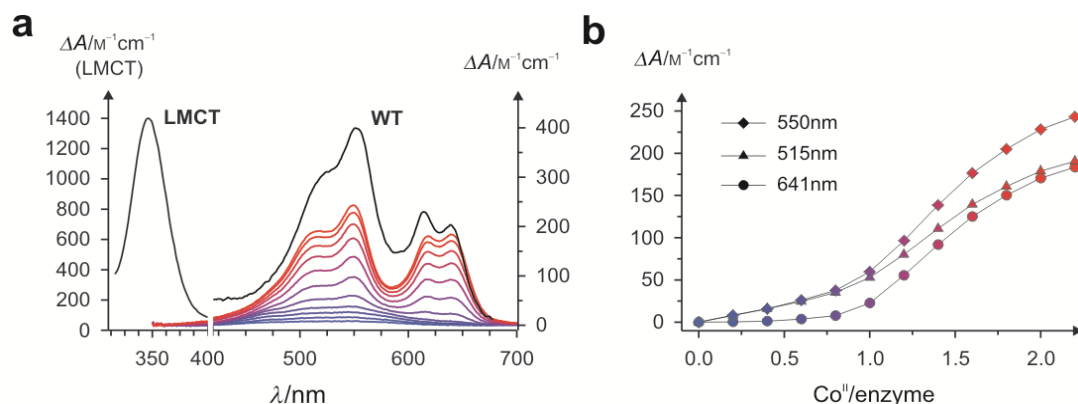
Supplementary Figure 5. Activity profile of apo-Cys221Asp BcII against nitrocefin upon addition of Zn^{II} (left) and Co^{II} (right), determined by stopped-flow measurements. Specific activity (v_0) is the initial rate of hydrolysis (in $\mu\text{M s}^{-1}$) per unit enzyme concentration (in μM). Reaction medium is 15 mM Hepes pH 7.5, 200 mM NaCl, 200 μM nitrocefin, stirred with Chelex 100, at 25 °C.



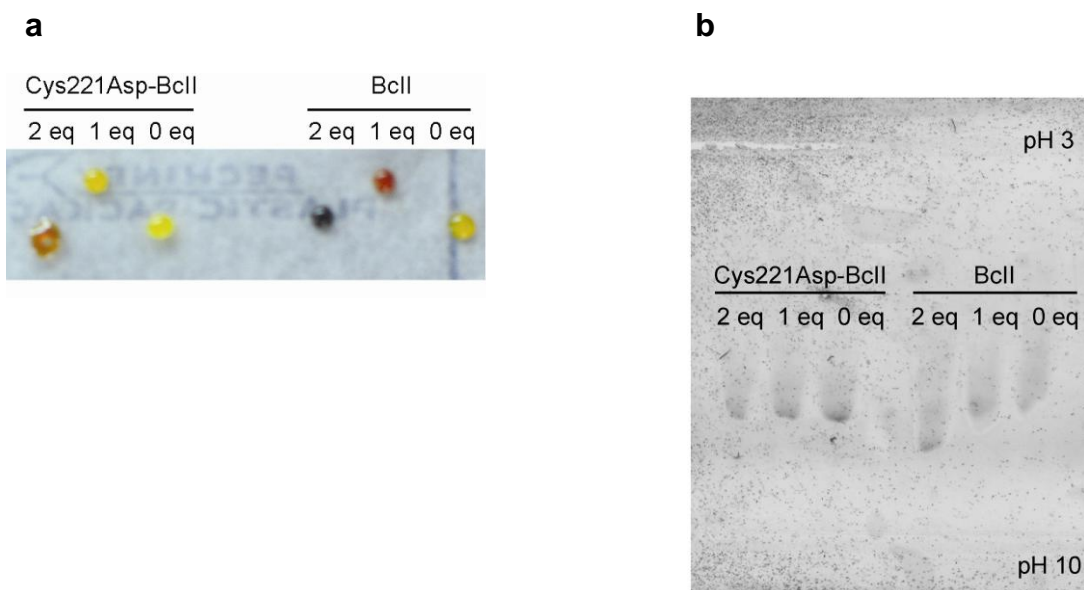
Supplementary Figure 6. Three-dimensional superposition of metal-binding sites of di-Zn^{II}BcII (PDB 3i13, *cyan*), and di-Zn^{II} Cys221Asp BcII (PDB 3kns, *wheat*, as obtained in this work). Numbers indicate the Zn^{II} ions. Dotted lines indicate selected non-covalent interactions. ACE is an acetate anion bound to Cys221Asp BcII mutant.



Supplementary Figure 7. Spectroscopic titrations performed on BcII-Cys221Asp following Co^{II}-substitution. (a) Difference spectra resulting from titration of the apoprotein with Co^{II}, recorded every 0.2 Co^{II} equivalents (blue to red, right axis). The spectrum of di-Co^{II}-BcII (WT, right axis) is included for comparison (black), adapted from Llarrull *et al.*¹⁶ The ligand-to-metal charge transfer (LMCT, left axis) absorption at 343 nm is absent in the mutant due to the Cys221Asp mutation. (b) Selected traces of peak absorptions (at 550 nm, 515 nm and 641 nm), highlighting distinct spectroscopic features for the mutant in the mono-Co^{II} and di-Co^{II} forms.



Supplementary Figure 8. Differentiation of apo, mono and di-metallic forms of BcII and BcII-Cys221Asp mutant. The apo forms of each protein were prepared by dialysis against chelating agents as previously described.⁷ Different aliquots of these samples in their apo forms were supplemented with 1 or 2 equivalents of Zn^{II}. (a) Mixing 2 μ l of each concentrated stock (50 μ M) with 1 μ l of nitrocefin (this colorimetric substrate changes from yellow to dark red when hydrolyzed) allowed detection of activity only in the cases of BcII supplemented with 2 or 1 equivalent and BcII-Cys221Asp supplemented with 1 Zn^{II} equivalent. (b) Isoelectric focusing was performed with a solution of ampholytes between pH 3 and 10. 1 μ g of the solutions with 2, 1 and 0 equivalent of added Zn^{II} were loaded. In the case of BcII-Cys221Asp, the mobility pattern does not allow to discriminate the apo, mono or di forms. However, wild type BcII appears to have a higher isoelectric point in the presence of two Zn^{II} equivalents as compared to the BcII-Cys221Asp mutant in the same conditions, suggesting a higher Zn^{II} content in the wt enzyme. We propose that Zn^{II} dissociation from the mutant results from its lower binding affinity, leading to metal loss upon dilution.



Supplementary Table 1. Steady-state kinetic parameters of BcII-Cys221Asp. Reaction medium was 15 mM Hepes pH 7.5, 200 mM NaCl and 100 μ M ZnSO₄ at 30 °C. Kinetic parameters shown for the wild-type enzyme obtained under similar reaction conditions were already reported by us¹. Substrates are cephaloridine (CLD), imipenem (IMI), cefotaxime (CTX), benzylpenicillin (PEN) and nitrocefin (NTR). Reported kinetic parameters correspond to the average of at least three replicates \pm s.d.

	k_{cat} (s^{-1})		K_{M} (μM)		$k_{\text{cat}}/K_{\text{M}}$ ($\mu\text{M}^{-1} \text{s}^{-1}$)		Ratio Cys221Asp/BcII
	Cys221Asp	BcII ¹	Cys221Asp	BcII ¹	Cys221Asp	BcII ¹	
CLD	429 \pm 41	57.9	2,560 \pm 390	1,250	0.168 \pm 0.0098	0.046	3.65
IMI	172 \pm 27	279	106 \pm 4.5	687	0.616 \pm 0.012	0.41	1.50
CTX	140 \pm 14	80.5	44.8 \pm 6.3	40	3.05 \pm 0.46	1.86	1.64
PEN	623 \pm 37	1,020	521 \pm 23	662	1.20 \pm 0.015	1.50	0.80
NTR	140 \pm 11	30	101 \pm 8.7	9.8	1.39 \pm 0.094	3.07	0.45

Supplementary Table 2. Dissociation constant values for the first (K_{d1}) and the second (K_{d2}) Zn^{II} binding event estimated by competition with PAR (4-(2-pyridylazo)-resorcinol). The data shown are the best fit value for each parameter \pm standard error. Fit of the experimental data for wild type BcII gave a K_{d1} value with a high error (Model I). We also fit the data to a model fixing the K_{d1} value to 10 nM (Model II) to analyze the possibility of cooperative binding. Model I and Model II are shown on Supplementary Methods.

		K_{d1} (nM)	K_{d2} (nM)
BcII	Model I	1.9 ± 3.3	8.6 ± 3.9
	Model II	10 (fixed)	4.3 ± 1.0
BcII-Cys221Asp	Model I	9.2 ± 1.7	267 ± 71

Supplementary Table 3. Data collection and refinement statistics

	Mono-Zn ^{II} BcII-Cys221Asp (PDB 3KNR)	Di-Zn ^{II} BcII-Cys221Asp (PDB 3KNS)
Data collection		
Space group	<i>P</i> 2 ₁	<i>P</i> 2 ₁
Cell dimensions		
<i>a</i> , <i>b</i> , <i>c</i> (Å)	80.14, 94.36, 79.90	79.78, 94.34, 79.78
β (°)	120.11	119.62
Resolution (Å)	23.3 (1.75) – 1.71*	23.3 (1.62) – 1.58
<i>R</i> _{merge}	0.043 (0.386)	0.040 (0.299)
<i>I</i> / σ <i>I</i>	33.9 (2.76)	33.5 (3.83)
Completeness (%)	96.8 (78.6)	94.5 (88.9)
Redundancy	3.1 (2.7)	3.8 (3.6)
Refinement		
Resolution (Å)	1.71	1.58
No. reflections	103,745	125,621
<i>R</i> _{work} / <i>R</i> _{free}	0.172 / 0.210	0.152 / 0.179
No. atoms		
Protein	6,500	6,457
Ligand/ion	4	8
Water	1,147	1,318
<i>B</i> -factors		
Protein	21.24	16.94
Ligand/ion	21.42	17.16
Water	24.27	20.78
R.m.s deviations		
Bond lengths (Å)	0.020	0.019
Bond angles (°)	1.793	1.664

*Highest resolution shell is shown in parenthesis.

Supplementary Methods

Plasmid construction and site-directed mutagenesis

The megaprimer method² was used to introduce the Cys221→Asp mutation. The mutagenic primer was 5'-GTTGGAGGCGATTTAGTGAAGTCGACGTCC-3' introducing a Cys221→Asp mutation (*bold*) and also a silent mutation introducing a *Sal* I restriction site (*underlined*). The external primers were 5'-CTATAAAAATAGGCGTATCACGAGG-3' (used in the first PCR) and 5'-GTACTTGTGGATTCTTCTTGGGATG-3' (used in the second PCR). The plasmid containing the wild-type *bcII* gene (pETβLIInew) was used as DNA template. Polymerase chain reactions were run using *Pfu* DNA polymerase (Promega).

The recombinant plasmid pETβLIInew contains the complete gene sequence of mature BcII protein (681 bp) linked in frame to the 3'-end *Schistosomajaponicus* glutathione S-transferase gene. A fragment containing the C-terminal sequence of the *bcII* gene was amplified by PCR using the following forward (5'-GTACTTGTGGATTCTTCTTGGGATG-3') and reverse (5'-CCTCTCTTTTGAAGCTTTACAATTTCTTAT-3') primers, introducing a *Hind*III restriction site (*underlined*) 10 bp downstream the *bcII* gene stop codon. The PCR product digested with *Pst*I and *Hind*III restriction enzymes was cloned with a 336 bp *Bam*HI-*Pst*I fragment containing the N-terminal region of BcII,³ between *Bam*HI and *Hind*III sites of the pETGEX-CT vector.⁴

The expression vector pET-Term contains the terminator sequence of *bcII* gene⁵ cloned into the expression vector pETGEX-CT.⁴ A 900 bp fragment, downstream of *bcII* gene, was amplified by PCR using the following forward (5'-AAGAAATTGTAAAGCTTCAAAGAGAGGAG-3') and reverse (5'-AAATGAATTCGTATACCCTAGCTGAGC-3') primers, introducing a *Hind*III site and *Eco*RI sites 5'- and 3'- respectively (*underlined*). The PCR product was cloned into *Hind*III and *Eco*RI sites of pETGEX-CT vector.

The pETBcII-Term and pETCYS221ASP-Term expression vectors contain the *bcII* and *bcII-CYS221ASP* gene sequences respectively cloned into the pET-Term vector.

The expression vectors pKP, pKP-BcII were available in the laboratory¹. The vector pKP-BcII-Cys221Asp was made replacing the *bcII* gene in pKP-BcII by *bcII-Cys221Asp* from pETBcII-Cys221Asp-Term, obtained through digestion of both plasmids with the restriction enzymes *Bam*HI and *Xho*I as described previously for pKP-BcII¹.

All plasmids sequences used in this work were checked by restriction patterns and DNA sequencing.

Determination of minimal inhibitory concentrations

The minimal inhibitory concentrations (MICs) for ampicillin and cefotaxime were determined by the standard agar macro dilution method.¹ *E. coli* JM109 cells were transformed with pKP (negative control) pKP-BcII and pKP-BcII-Cys221Asp vectors. The pKP-BcII and pKP-BcII-Cys221Asp plasmids contain the *bcII* and *bcII-Cys221Asp* genes respectively, linked to the leader sequence *pelB* from pectatelyase, in order to target the corresponding enzymes to the periplasm. Single colonies from each transformation were grown in liquid media overnight (LB with 50 mg/ml kanamycin, Kan) at 37 °C with shaking. The saturated cultures were diluted 200 times into fresh media, grown to OD₆₀₀ ~ 0.1, adjusted to OD₆₀₀ = 0.01 and plated on selective media LB agar with 50µg/ml kanamycin, 0.5 mM isopropyl β-D-galactopyranoside (IPTG) and variable amounts of ampicillin (0- 1024 µg/ml) or cefotaxime (0 - 32 µg/ml). The plates were incubated overnight at 37 °C and the MICs were determined form at least 3 independent experiments.

Evaluation of the antibiotic sensitivity against different Zn^{II} concentrations

E. coli JM109 cells transformed with pKP (negative control), pKP-BcII and pKP-BcII-Cys221Asp vectors were used to evaluate the antibiotic resistance against different Zn^{II} concentrations. Overnight saturated cell cultures, grown in LB with 50 µg/ml Kan at 37°C with shaking, were serially diluted and plated on LB agar with 50 µg/ml Kan, 0.5 mM IPTG, and variable amounts of ampicillin or cefotaxime and 5 µM EDTA (low Zn^{II}), without extra Zn^{II}, and 250 µM Zn^{II} (excess Zn^{II}, as ZnSO₄). Then, the plates were incubated overnight at 37 °C.

Periplasmic extracts and Western blot analysis

E. coli JM109 cells transformed with pKP (negative control), pKP-BcII or pKP-BcII-Cys221Asp vectors were used to evaluate the periplasmic wild-type BcII or BcII-Cys221Asp levels by Western blot, as it was described previously.⁶ Periplasmic extracts were obtained by isosmotic shock with lysozyme and the total proteins were resolved by 12% SDS-PAGE. The proteins were transferred to a nitrocellulose membrane and the wild-type BcII or BcII-

Cys221Asp proteins were identified by rabbit polyclonal antibodies against BcII as described by Orellano *et al.*³ The reactivity of the anti-BcII polyclonal antibodies was tested for both proteins by using different amounts of purified protein and measuring the intensity of each band by densitometry. The Integrated Optical Density (IOD) of each band was normalized to the band with 62.5 ng in the same assay (internal control).

Activity measurements with periplasmic extracts

Traditional methods of periplasmic purification commonly use lysozyme and EDTA. These protocols cannot be applied to our system if activity is to be measured, since the presence of the chelating agent alters the metal content of the enzyme and, consequently, the enzyme activity.

Therefore, we employed an alternative protocol to prepare periplasmic fractions, avoiding the use of EDTA and lysozyme²¹. Briefly, 5 ml of induced cell culture expressing wt BcII or BcII-Cys221Asp at OD 1.5 were first resuspended in 30 mM Tris, 20 % sucrose buffer (pH 8.0), and then were subjected to osmotic shock with 2 ml of cold 5 mM MgSO₄. With these periplasmic extracts we measured initial velocities of cefotaxime hydrolysis at saturating substrate concentration (200 μM). Reaction mediums tested were: 15mM Hepes pH 7.5, 200 mM NaCl at 30 °C, previously stirred with Chelex 100, and the same supplemented with 20 μM Zn^{II}. Activity measurements were repeated with three different periplasmic preparations.

Periplasmic extracts were concentrated 20-fold with Amicon Ultra centrifugal filters MWCO10 kDa and 15 μl were loaded on SDS-PAGE gels, known quantities of purified proteins were loaded for calibration. Based on quantification from Western blot assays, the final enzyme concentration to measure activity on the cuvette was approximately 2 nM.

Protein expression, purification and sample preparation

BcII-Cys221Asp was expressed and purified following the protocol for wild-type BcII,³ using the pETBcII-Cys221Asp-Term expression vector. Apo-enzymes and cobalt derivatives were prepared as previously reported by us.⁷ Protein samples were quantified spectrophotometrically, using a molar extinction coefficient of 30,500 M⁻¹ cm⁻¹.⁸

Steady-state kinetic measurements

Kinetic parameters were determined spectrophotometrically through nonlinear fitting of complete reaction time-courses with the integrated Michaelis-Menten model. Reaction medium

is 15 mM Hepes pH 7.5, 200 mM NaCl and 100 μM ZnSO_4 at 30 °C. Differential molar extinction coefficients for antibiotic hydrolysis are $\Delta\epsilon_{260\text{nm}} = -13,600 \text{ M}^{-1} \text{ cm}^{-1}$ (cephaloridine)¹, $\Delta\epsilon_{300\text{nm}} = -9,000 \text{ M}^{-1} \text{ cm}^{-1}$ (imipenem)⁹, $\Delta\epsilon_{262\text{nm}} = -7,500 \text{ M}^{-1} \text{ cm}^{-1}$ (cefotaxime)¹, $\Delta\epsilon_{235\text{nm}} = -800 \text{ M}^{-1} \text{ cm}^{-1}$ (benzylpenicillin)¹⁰ and $\Delta\epsilon_{485\text{nm}} = 17,420 \text{ M}^{-1} \text{ cm}^{-1}$ (nitrocefim)¹¹. All the antibiotics used were from SIGMA, with the exception of Imipenem (USP Pharmacopeia) and Nitrocefim (OXOID), and all of them had a purity > 95%.

Reported kinetic parameters correspond to the average of at least three replicates \pm s.d.

Zn titration of purified enzymes followed by activity and estimation of K_{act}

The initial velocities measurements for cefotaxime 200 μM were determined spectrophotometrically for wild-type BcII and BcII-Cys221Asp in the presence of increasing concentration of added ZnCl_2 (from an atomic standard absorption solution). Aliquots from stocks of 60 μM holo-enzyme or apo-enzyme diluted to 2 nM were used to initiate the reaction. Reaction medium was 15mM Hepes pH 7.5, 200 mM NaCl at 30 °C, previously stirred with Chelex 100. Differential molar extinction coefficients for antibiotic hydrolysis: $\Delta\epsilon_{262\text{nm}} = -7,500 \text{ M}^{-1} \text{ cm}^{-1}$ (cefotaxime)¹.

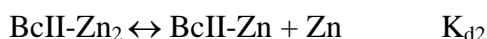
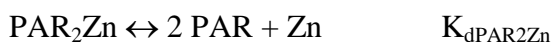
There were no differences between experimental points performed with holo or apo-enzymes stocks, since equilibrium is established once the protein is diluted. The initial velocities values were relativized to the value at 100 μM ZnCl_2 (considered as the maximum activity). The experimental data was fit to one Zn^{II} binding event that accounts for the enzymes activation, and activation constants (K_{act}) were determined using the DynaFit software¹².



Metal binding affinities measured by competition with 4-(2-pyridylazo)-resorcinol (PAR)

The dissociation constants were estimated from competition experiments with the chromophoric chelator 4-(2-pyridylazo)-resorcinol (PAR; from Sigma). The indicator was first titrated with Zn^{II} at 25 °C, and changes in absorbance at 414 nm (absorption maxima for PAR) and 500 nm (absorption maxima for the complex $\text{PAR}_2(\text{Zn})$) were fit with DynaFit software¹² to obtain the dissociation constant of Zn^{II} from the complex with PAR (PAR_2Zn) in 40 mM MOPS, pH 7.3, 0.1 M NaCl (previously stirred with Chelex 100), at 25 °C. A value of $(2.6 \pm 0.2) \times 10^{-12}$

M^2 was obtained, with $\epsilon_{\text{PAR}414\text{nm}} = 36868 \pm 1843 \text{ M}^{-1} \text{ cm}^{-1}$, $\epsilon_{\text{PAR}500\text{nm}} = 1289 \pm 65 \text{ M}^{-1} \text{ cm}^{-1}$, $\epsilon_{\text{PAR}2\text{Zn}414\text{nm}} = 12788 \pm 576 \text{ M}^{-1} \text{ cm}^{-1}$, $\epsilon_{\text{PAR}2\text{Zn}500\text{nm}} = 80000 \pm 4000 \text{ M}^{-1} \text{ cm}^{-1}$. Afterward, solutions of 3 and 6 μM PAR were titrated with 0.1–3 μM apo-wild-type BcII or apo-BcIICys221Asp in the presence of 1.25 μM ZnCl_2 (from an atomic standard absorption solution from SIGMA), in the same reaction conditions. Each point was repeated three times and their spectrums were recorded from 320 to 600 nm. The changes in absorbance at 414 nm and 500 nm with added apo-protein (taking the average for each point), obtained for both PAR concentrations, were fit together to the following model (Model I) using the DynaFit software¹², in order to calculate K_{d1} and K_{d2} ($K_{d\text{PAR}2\text{Zn}}$ was fixed to the value determined previously):



For wild-type BcII, as K_{d1} could not be determined accurately, a model with its value fixed at 10 nM (Model II) was also tested to analyze the possibility of cooperative binding.

BcII-Cys221Asp activity against the chromogenic cephalosporin substrate nitrocefin in the course of titration with Zn^{II} or Co^{II}

A rapid-mixing stopped-flow unit (RX2000, Applied Photophysics) was attached to a spectrophotometer (V-550, Jasco), and employed to measure initial rates of nitrocefin hydrolysis mediated by BcII-Cys221Asp in the presence of increasing metal concentrations. A 0.5 ml aliquot of 400 μM nitrocefin in buffer A (15 mM Hepes pH 7.5, 200 mM NaCl, stirred with Chelex 100 to remove divalent cations), was mixed with a 0.5 ml aliquot of enzyme sample (a 50 ml solution of 1 μM apoenzyme in buffer A, added with 5 μl aliquots of 1.0 M ZnSO_4 or 1.0 M CoSO_4), and the absorbance at 485 nm was then recorded and stored for data processing. Temperature was kept at 25 °C with a Lauda RC-6 water circulator. This procedure was repeated iteratively until activity reached a plateau value. Finally, the corresponding corrections for dilution effects were applied.

Activity against imipenem of mono- and di-Co^{II} BcII-Cys221Asp detected through photodiode-array stopped-flow measurements

Ligand-field absorption bands of Co^{II}-substituted BcII-Cys221Ap were analyzed by electronic spectroscopy photodiode-array stopped-flow measurements (SX18-MVR, Applied Photophysics). Temperature was kept at 7 °C with a Lauda RC-6 water circulator. Reaction medium was 100 mM Hepes pH 7.5, 200 mM NaCl, stirred with Chelex 100 to remove divalent cations. The activity assays were performed in two conditions: 0.70 Co^{II} equivalents (mixing apoprotein and CoSO₄ at 467 μM and 327 μM, respectively), corresponding to the mono-Co^{II} form, and 2.8 Co^{II} equivalents (mixing apoprotein and CoSO₄ at 326 μM and 913 μM, respectively), corresponding to the di-Co^{II} form. Taking into account that the protein and Co^{II} concentrations used in these assays are significantly higher than the dissociation constants for Co^{II}, the condition at 0.7 Co^{II} eq can be assumed to contain 327 μM of the mono-Co^{II} species, *ie.*, the same as that of Co^{II}, the limiting reagent in these conditions. The same holds true for the condition at 2.8 Co^{II} eq, *ie.*, the di-Co^{II} species concentration is the same as that of the apoprotein, the limiting reagent in this case. Each enzyme sample was rapidly mixed in a 1:1 ratio with a solution of 5 mM imipenem, resulting in mixture of 163 μM for both mono- and di-Co^{II} species, and 2.5 mM imipenem. Absorption spectra were then recorded for a path-length of 0.2 cm, and stored for data processing.

Determination of crystal structures

BcII-Cys221Asp mutant crystals were grown using the hanging-drop vapor-diffusion method, in VDX multi-well (Hampton) plates with 300 μl reservoir solutions. Single crystals grew after a period of two weeks at 20°C. The reservoir solution contained 0.1 M sodium acetate pH 4.9 and 2.8 M ammonium sulfate. Drops consisted of 2 μl protein solution (2 mg/ml in 10 mM Tris-HCl pH 7.0) and 2 μl reservoir solution, supplemented with 1 mM or 20 mM ZnSO₄, in which *P*2₁ space group crystals grew containing one and two Zn^{II} ions per monomer, respectively. Crystals were soaked in a cryoprotectant solution prepared with the mother liquor together with 18 % (v/v) of glycerol, mounted in nylon loops and flash-cooled in liquid nitrogen.

Diffraction data was collected in the D03B-MX1 beamline at LNLS (Campinas, Brazil), and processed with HKL2000¹³ and the CCP4 Suite of programs.¹⁴ Phasing was conducted by molecular replacement with the program AMORE¹⁵, using the structure of BcII (PDB 1bc2) as

phasing model. Refinement was performed with REFMAC 5.2¹⁶. Manual building was conducted with COOT¹⁷ and TURBO-FRODO¹⁸, using σ_A -weighted $2F_O - F_C$ and $F_O - F_C$ electron density maps. Structure validation was realized with PROCHECK¹⁹ and COOT. Figures were prepared with PyMOL 0.99rc6.²⁰

Differentiation of apo, mono and dimetallic forms of BcII and Cys221Asp-BcII mutant

The apo forms of each protein were prepared by dialysis against chelating agents as previously described.⁷ Different aliquots of these samples in their apo forms were supplemented with 1 or 2 equivalents of Zn^{II}. A first test of these preparations was performed mixing 2 μ l of each concentrated stock (50 μ M) with 1 μ l of nitrocefin (this colorimetric substrate changes from yellow to dark red when hydrolyzed). This experiments allowed to test that reconstitution of the enzyme activity was feasible in both samples.

Isoelectric focusing was performed with the Model 111 Mini IEF Cell from Biorad, following its instruction for polyacrilamide gels. A solution of ampholytes between pH 3 and 10 was used and 1 μ g of the solutions with 2, 1 and 0 equivalent of added Zn^{II} were loaded. Focusing was carried out at 100 V for 15 minutes, 200 V for 15 minutes and 450 V for 60 minutes. Proteins were detected by staining with Coomassie Blue G-250.

Supplementary References

1. Tomatis,P.E., Rasia,R.M., Segovia,L., & Vila,A.J. Mimicking natural evolution in metallo-beta-lactamases through second-shell ligand mutations. *Proc. Natl. Acad. Sci. U. S. A* **102**, 13761-13766 (2005).
2. Sarkar,G. & Sommer,S.S. The megaprimer method of site-directed mutagenesis. *Biotechniques* **8**, 404-407. 1990.
3. Orellano,E.G., Girardini,J.E., Cricco,J.A., Ceccarelli,E.A., & Vila,A.J. Spectroscopic characterization of a binuclear metal site in *Bacillus cereus* beta-lactamase II. *Biochemistry* **37**, 10173-10180 (1998).
4. Sharrocks,A.D. A T7 expression vector for producing N- and C-terminal fusion proteins with glutathione S-transferase. *Gen* **138**, 105-108 (1994).
5. Hussain,M., Carlino,A., Madonna,M.J., & Lampen,J.O. Cloning and sequencing of the metallothioprotein beta-lactamase II gene of *Bacillus cereus* 569/H in *E.coli*. *J. Bacteriol.* **164**, 223-229 (1985).
6. Moran-Barrio,J., Limansky,A.S., & Viale,A.M. Secretion of GOB metallo-beta-lactamase in *Escherichia coli* depends strictly on the cooperation between the cytoplasmic DnaK chaperone system and the Sec machinery: completion of folding and Zn(II) ion acquisition occur in the bacterial periplasm. *Antimicrob. Agents Chemother.***53**, 2908-2917 (2009).
7. Llarrull,L.I., Tioni,M.F., Kowalski,J., Bennett,B., & Vila,A.J. Evidence for a dinuclear active site in the metallo-beta-lactamase BcII with substoichiometric Co(II). A new model for metal uptake. *J Biol. Chem.* **282**, 30586-30595 (2007).
8. Paul-Soto,R. *et al.* Mono- and binuclear Zn²⁺-beta-lactamase. Role of the conserved cysteine in the catalytic mechanism. *J. Biol. Chem.* **274**, 13242-13249 (1999).
9. Felici,A. *et al.* An overview of the kinetic parameters of class B beta-lactamases. *Biochem. J.* **291**, 151-155 (1993).
10. Rasia,R.M. & Vila,A.J. Exploring the role and the binding affinity of a second zinc equivalent in *B. cereus* metallo-beta-lactamase. *Biochemistry* **41**, 1853-1860 (2002).
11. Crowder,M.W., Wang,Z., Franklin,S.L., Zovinka,E.P., & Benkovic,S.J. Characterization of the metal binding sites of the beta-lactamase from *Bacteroides fragilis*. *Biochemistry* **35**, 12126-12132 (1996).
12. Kuzmic,P. Program DYNAFIT for the analysis of enzyme kinetic data: Application to HIV proteinase. *Anal. Biochem.* **237**, 260-273 (1996).
13. Otwinowski,Z. & Minor,W. Processing of X-ray diffraction data collected in oscillation mode. *Methods Enzymol.* **276**, 307-325 (1997).

14. Collaborative Computational Project Number 4 The CCP4 suite: programs for protein crystallography. *Acta Crystallogr. D. Biol. Crystallogr.* **50**, 760-763 (1994).
15. Navaza, J. AMoRe: an automated package for molecular replacement. *Acta Crystallogr. D. Biol. Crystallogr.* **55**, 247-255 (1994).
16. Murshudov, G.N., Vagin, A.A., & Dodson, E.J. Refinement of macromolecular structures by the maximum-likelihood method. *Acta Crystallogr. D. Biol. Crystallogr.* **53**, 240-255 (1997).
17. Emsley, P., Lohkamp, B., Scott, W.G., & Cowtan, K. Features and development of Coot. *Acta Crystallogr. D. Biol. Crystallogr.* **66**, 486-501 (2010).
18. Roussel, A. & Cambilleau, C. TURBOFRODO. 1992. LCCMB, Marseille, France, Biographics.
19. Laskowski, R.A., Mac Arthur, M.W., Moss, D.S., & Thornton, J.M. PROCHECK: a program to check the stereochemical quality of protein structures. *J. Appl. Cryst.* **26**, 283-291 (1993).
20. DeLano, W.L. The PyMOL Molecular Graphics System. 2002. DeLano Scientific, San Carlos, CA.
21. Tomatis, P.E., Fabiane, S.M., Simona, F., Carloni, P., Sutton, B.J., and Vila, A.J. Adaptive protein evolution grants organismal fitness by improving catalysis and flexibility. *Proc. Natl. Acad. Sci. U. S. A* 105:20605-20610 (2008).